pubs.acs.org/acschemicalbiology

Article

Origin of the Different Binding Affinities of (9*R*)- and (9*S*)-Hexahydrocannabinol (HHC) for the CB_1 and CB_2 Cannabinoid Receptors

Pan-Pan Chen, Meng Duan, Qingyang Zhou, Fang Liu, Yi Tang,* Neil K. Garg,* and K. N. Houk*

Cite This: https://doi.org/10.1021/acschembio.5c00399

Read Online

ACCESS | Metrics & More | Article Recommendations | Supporting Information

ABSTRACT: Hexahydrocannabinols (HHCs) are emerging cannabinoids that have become available for recreational use and were recently classified as Schedule II under an international treaty. Although often advertised for having desirable effects, recent studies have shown that commercial products typically contain variable amounts of two epimers, (9*R*)-HHC and (9*S*)-HHC. In turn, these epimers have been shown to have different binding affinities to the CB_1 and CB_2 receptors. We report a computational study that interrogates the origins of these differing affinities. Molecular docking and molecular dynamics simulations were employed to investigate the binding of (9*R*)-HHC and (9*S*)-HHC to cannabinoid receptors CB_1 and CB_2. Computational results show key binding interactions and highlight important conformational effects. For both receptors, the (9*R*)-HHC isomer exists primarily in a chair conformation, placing the C9 methyl substituent in a favorable equatorial position in the active sites. However, (9*S*)-HHC exists in equilibrium between the chair and twist-boat conformations within the receptor's active site, ultimately leading to less favorable binding in the CB_1 and CB_2 active sites, making (9*S*)-HHC a less favorable ligand compared to (9*R*)-HHC. These studies explain the relative binding of HHCs and are expected to enable the investigation of other cannabinoids that display improved or selective receptor binding.

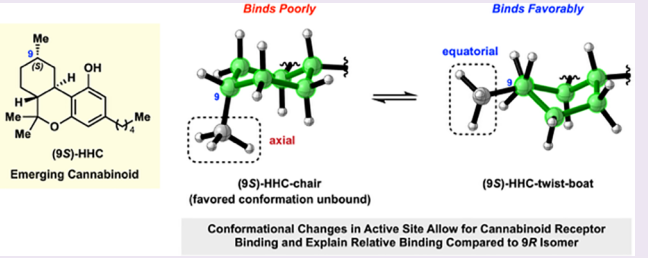

INTRODUCTION

The recent legalization and decriminalization of marijuana and related cannabis products in the majority of the United States and elsewhere have led to a growing societal impact.[1−5] One notable area pertains to so-called emerging cannabinoids, which are typically derivatives or analogs of Δ^9-tetrahydrocannabinol (Δ^9-THC) that have become available for recreational use.[6−9] Emerging cannabinoids are generally understudied, with the pace of scientific research often lagging behind the availability of new cannabis products to consumers. Thus, it is vital that fundamental science be prioritized as a means to evaluate new and emerging cannabinoids.[10]

An especially prominent class of emerging cannabinoids is hexahydrocannabinols (HHCs), with two major compounds being the most common.[11−18] These are (9*R*)-HHC and (9*S*)-HHC (Figure 1), typically derived by reduction of Δ^8- or Δ^9-THC. Whereas Δ^9-THC is readily available as the primary psychoactive component of marijuana, Δ^8-THC has become prominent following the 2018 Farm Bill, presumably made by acid-catalyzed cyclization of cannabidiol (CBD).[6−9,19] Commercial HHC products are often advertised as being an attractive product for consumers, but a recent study highlights that the ratio of isomers in marketed products is highly variable.[11] This is notable, as recent studies have shown that (9*R*)-HHC and (9*S*)-HHC have very different binding affinities to the two cannabinoid receptors, CB_1 and CB_2, leading to variable levels of bioactivity.[16,20−22] CB_1 receptors are primarily in the brain and mediate psychoactive effects, while CB_2 receptors are mainly in the immune system and regulate inflammation. Generally speaking, the activity of (9*R*)-HHC is on par with that of Δ^9-THC, while the activity of (9*S*)-HHC is roughly ten times less.[11] In a recent meeting of the United Nations Commission on Narcotic Drugs, HHC was placed under "Schedule II" of the 1971 Convention on Psychotropic Substances, effectively banning the compound under international treaty (although excluding the United States).[15]

In light of the societal impact of HHCs, we sought to examine the binding of these compounds to the CB_1 and CB_2 receptors in silico. We have now used modern density functional theory, molecular dynamics, and calculations of binding affinities to explore the structures and conformations of the HHC isomers as they bind to the cannabinoid

Received: May 25, 2025
Revised: July 12, 2025
Accepted: July 14, 2025

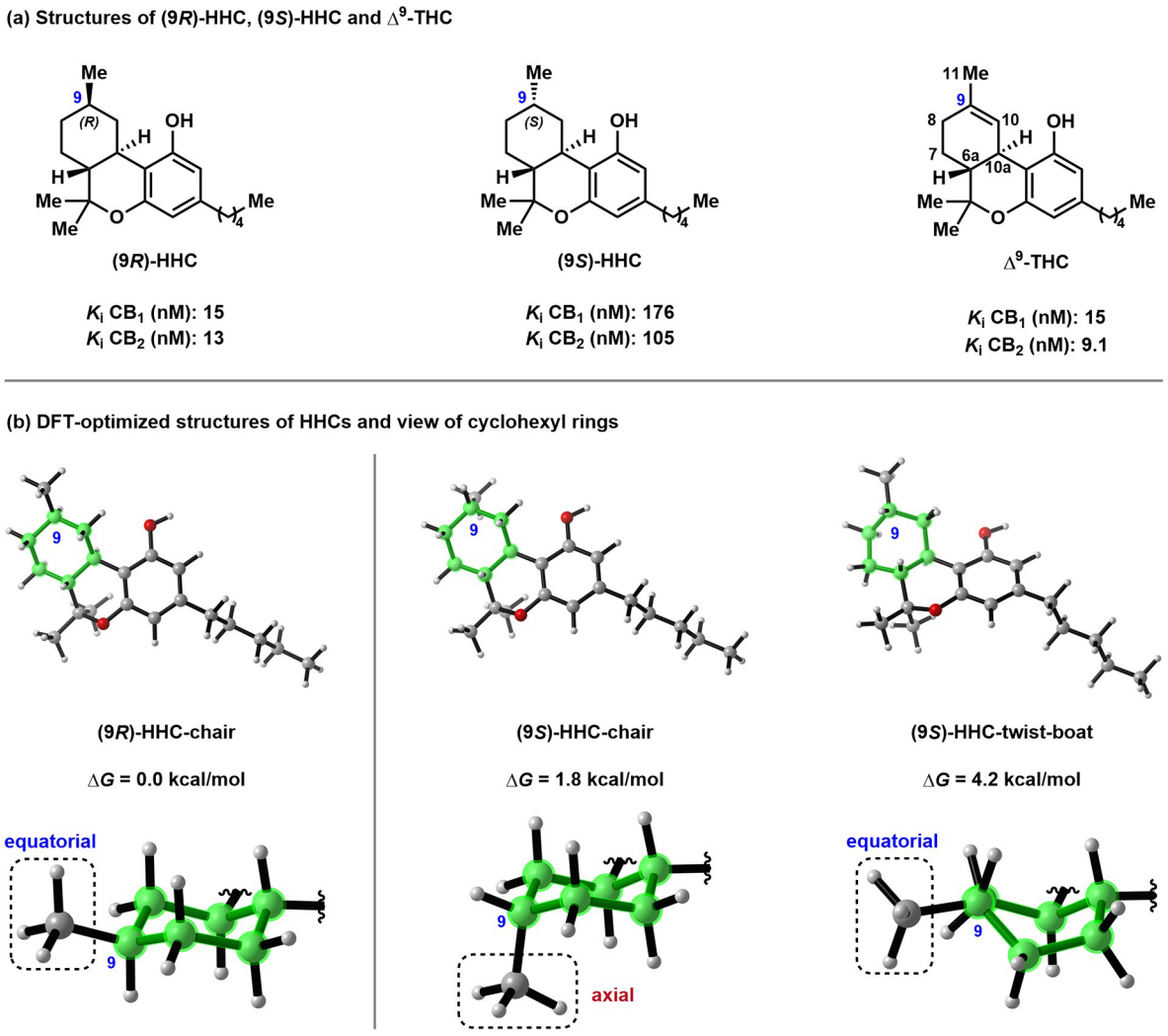

Figure 1. (a) (9*R*)-HHC, (9*S*)-HHC and Δ^9-THC, and their experimentally determined binding affinity to cannabinoid receptors. (b) DFT-optimized structures of HHCs highlighting the cyclohexyl ring conformation and the orientation of the C9 methyl substituent for each structure. For the depiction of the cyclohexyl rings, atoms of the parent structures are omitted for the sake of clarity.

receptors.[23] We find that the binding mode for the (9*R*)-HHC isomer of HHC is similar to that of THC, which explains their comparable binding affinities. For the (9*S*)-HHC isomer, we find there are subtle conformational changes in the binding pockets that are ultimately responsible for (9*S*)-HHC's inferior binding affinity. These effects are discussed herein.

RESULTS AND DISCUSSION

Conformation Studies of HHC Isomers. We initiated these studies by considering the conformations of (9*R*)-HHC and (9*S*)-HHC, before performing docking studies. Prior conformational studies of HHCs have been performed using NMR spectroscopy and calculations.[11,24−26] These key contributions suggest the importance of the C9 methyl group's orientation, analogous to earlier cannabinoid studies by Mechoulam et al.,[27] and hint at the possibility of there being important conformational effects.

Figure 1b shows the structures of (9*R*)-HHC and (9*S*)-HHC, as optimized quantum mechanically with the Truhlar density functional, M06-2X.[28,29] The 3D diagrams of molecules were generated using CYLView.[30] In (9*R*)-HHC, the cyclohexyl ring is in a chair conformation with the C9 methyl group being positioned equatorial. In the lowest energy conformer of (9*S*)-HHC, the cyclohexyl ring remains in a chair conformation, resulting in the C9 methyl group being oriented axially. The (9*S*)-HHC isomer (axial C9 methyl) is 1.8 kcal/mol higher in energy than (9*R*)-HHC (equatorial C9 methyl), consistent with the A-value of Me, 1.7 kcal/mol.[31] For (9*S*)-HHC, we also evaluated the twist-boat conformer, which positions the C9 methyl group in an equatorial orientation. This twist-boat conformer is 2.4 kcal/mol higher in energy compared to the chair conformer,[32] rendering it highly disfavored. As discussed below, we propose that these conformational effects are intimately tied to cannabinoid receptor binding.

The superimposed three-dimensional structures of the two HHC epimers, in their lowest energy conformations, and Δ^9-THC are shown in Figure 2. These overlays underscore the cyclohexyl ring conformations and the orientation of the C9 methyl group. In (9*R*)-HHC, the equatorial methyl group is located in a comparable position to the C9 methyl group of Δ^9-THC. However, in the (9*S*)-HHC epimer (favorable chair conformation), the axial methyl group protrudes from the bottom face of the quasiplanar alicyclic system. Although this

https://doi.org/10.1021/acschembio.5c00399
ACS Chem. Biol. XXXX, XXX, XXX−XXX

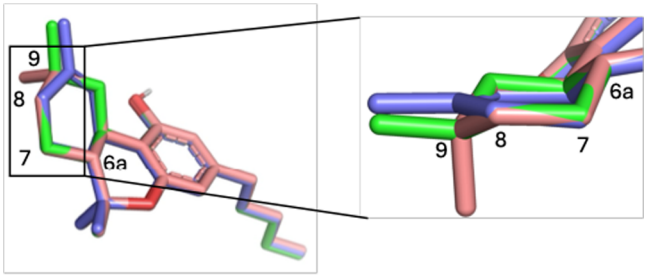

Figure 2. Overlays of DFT-optimized structures of (9*R*)-HHC (green; the C9 methyl group is equatorial), Δ^9-THC (blue; the C9 methyl group is equatorial), and (9*S*)-HHC-chair (pink; the C9 methyl group is axial). Nonpolar hydrogen atoms are omitted for clarity.

analysis provides a cursory explanation for the comparable binding affinity of (9*R*)-HHC to Δ^9-THC (and differing binding affinity for (9*S*)-HHC), we sought a more quantitative evaluation of receptor binding and to understand the differences in receptor binding for the two HHC isomers.

Docking Studies. As crystal structures of the human CB_1 and CB_2 receptors have only been disclosed within the past decade or less,[10,33,34] docking studies and molecular dynamics simulation studies of Δ^9-THC or its derivatives are sparse.[10,33,35−38] However, computational studies could improve our understanding of how THC derivatives bind to the CB_1 and CB_2 receptor active sites, which in turn could facilitate the design and discovery of improved or selective binders with therapeutic benefits. With regard to HHCs, one computational study was reported in 2024, where only the chair conformers of (9*R*)- and (9*S*)-HHC were evaluated in the CB_1 active site.[39] The study attributed the weak agonist property and low CB_1 affinity of (9*S*)-HHC to its lack of polar interaction with S383. The study ultimately concluded that the (9*S*)-HHC isomer binds through its chair conformer (axial C9 methyl group) in the active site by adopting an entirely different orientation compared to what is seen for Δ^9-THC and (9*R*)-HHC. The twist-boat conformer of (9*S*)-HHC was not discussed, and the corresponding computational studies for the CB_2 receptor active sites have not yet been reported.

We employed molecular docking studies to investigate the binding features of the HHC isomers in the cannabinoid receptor (i.e., both CB_1 and CB_2) active sites. Figure 3a shows the binding pose of the ligands (9*R*)-HHC (chair conformer) and (9*S*)-HHC (chair and twist-boat conformer) to the CB_1 receptor, whereas Figure 3b focuses on CB_2. The docking studies were performed with AutoDock Vina.[40,41]

Beginning with the chair conformers of (9*R*)-HHC (equatorial C9 methyl group) and (9*S*)-HHC (axial C9 methyl group), both are stabilized in the CB_1 active site through hydrogen bonding with S383 and aryl−aryl T-interactions with F170 and F268 (Figure 3a). The van der Waals radius of hydrogen is 1.2 Å and that of carbon is 1.75 Å, so when the C−H bond distance is about 2.9−3.0 Å, the interaction is attractive, but when shorter, the interaction becomes repulsive. When the H−H bond distance is less than 2.4 Å, the reaction is repulsive. As a result, the steric effect (shorter CH−C distance is 2.3 Å, and CH−H distance is 2.0 Å) between the axial methyl of (9*S*)-HHC (pink) and two nearby residues, F177 and H178, makes (9*S*)-HHC less favorable compared to (9*R*)-HHC (CH−C1 distance is 3.0 Å). That is, the axial methyl in (9*S*)-HHC interacts repulsively with the F177 and H178 residues (Figure 3a).

We also studied the docking of the twist-boat form of (9*S*)-HHC (equatorial C9 methyl group) (Figure 3a, yellow structure) in the CB_1 receptor. As anticipated, the steric hindrance encountered in the chair conformer of (9*S*)-HHC is alleviated in its twist-boat form, as the repulsive interactions involving the C9 methyl group and F177 and H178 are minimized in the twist-boat form (equatorial methyl). Hydrogen bonding O−O distances are 2.8−3.0 Å (phenol oxygen of HHC to oxygen of residue S383), which is important for receptor binding. Overall, the docking features of the twist-boat form of (9*S*)-HHC are very reminiscent of how (9*R*)-HHC binds the CB_1 receptor.

For the CB_2 receptor, the binding poses of (9*R*)-HHC (chair; equatorial C9 methyl group), (9*S*)-HHC (chair; axial

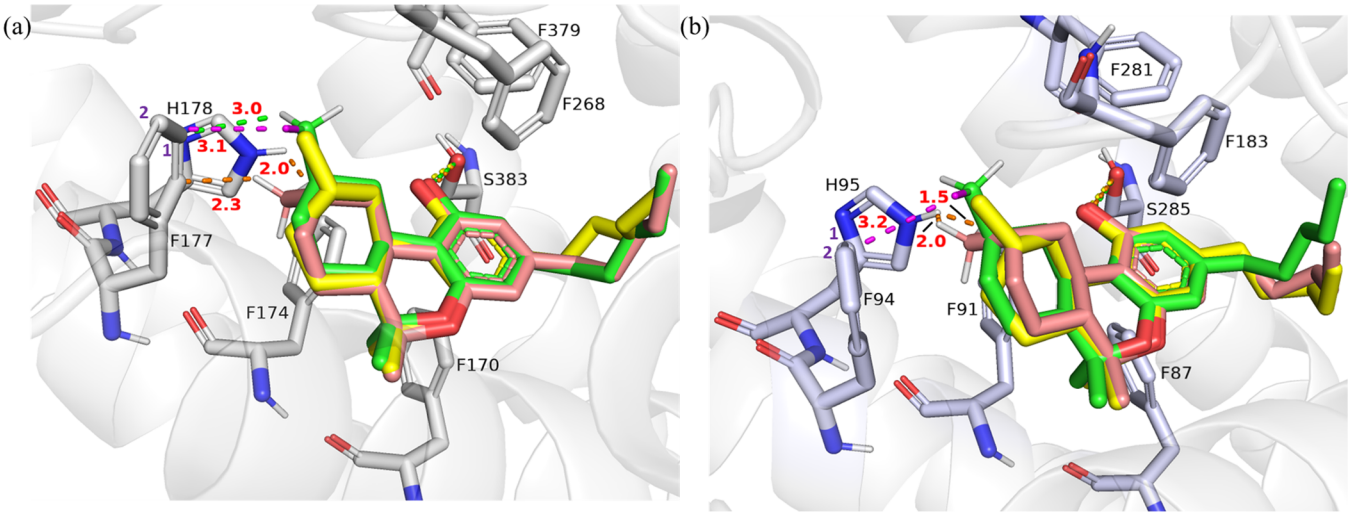

Figure 3. Molecular docking of (9*R*)-HHC (equatorial C9 methyl), (9*S*)-HHC-chair (axial C9 methyl) and (9*S*)-HHC-twist-boat (equatorial C9 methyl) in the active sites of (a) CB_1, (b) CB_2. Green: (9*R*)-HHC; Pink: (9*S*)-HHC-chair; Yellow: (9*S*)-HHC-twist-boat. Distances are given in Å, and nonrelevant hydrogens are omitted for clarity in panels (a) and (b). CH−π interaction (indicated by a magenta dashed line) distances were calculated from the methyl proton of (9*R*)-HHC to the center of the C1−C2 π-bond in both CB_1 and CB_2 cases.

https://doi.org/10.1021/acschembio.5c00399
ACS Chem. Biol. XXXX, XXX, XXX−XXX

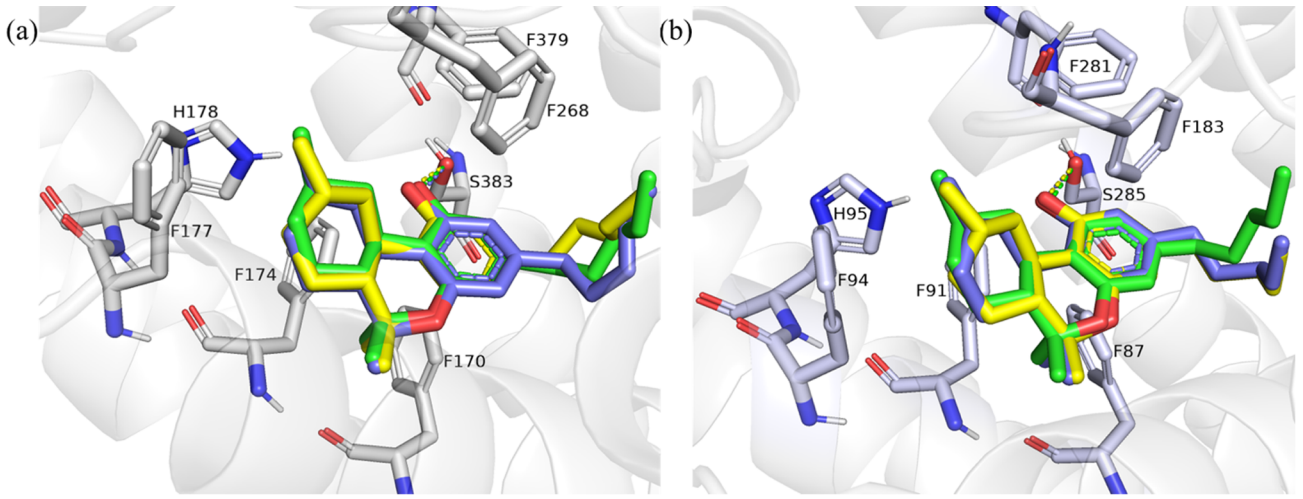

Figure 4. Molecular docking of (9*R*)-HHC (chair; equatorial C9 methyl), (9*S*)-HHC-twist-boat (equatorial C9 methyl), and Δ^9-THC (equatorial C9 methyl) in the active sites of (a) CB_1, and (b) CB_2. Green: (9*R*)-HHC; Yellow: (9*S*)-HHC-twist-boat; Blue: Δ^9-THC. Hydrogen bonding O−O distances are 2.8−3.0 Å for CB_1 case, and 3.1−3.3 Å for CB_2 case. Nonrelevant hydrogens are omitted for clarity in panels (a) and (b).

C9 methyl group), and the twist-boat conformer of (9*S*)-HHC (equatorial C9 methyl group) are very similar to those observed for the CB_1 receptor (Figure 3b). This is consistent with recent structural studies, which revealed that the two cannabinoid receptors (CB_1 and CB_2) share a conserved orthostatic binding pocket for their agonists. Notably, an additional allosteric binding pocket was identified for the CB_1 receptor.[42] The docked structures show that for all three substrates, the hydrogen-bonding (OH group of S285) and aryl−aryl T-interactions (aryl group of F183 and F87) stabilize the ligand in the active site of CB_2. The key steric repulsion in the CB_2 active site is with H95, instead of with F177 and H178 in CB_1. The binding of the chair conformer of (9*S*)-HHC (axial C9 methyl group) is disfavored, as seen by the short H−H bond distances of 2.0 and 1.5 Å between the hydrogens on the axial methyl group and the hydrogen of H95. In a comparison of the two conformers of (9*S*)-HHC, steric repulsion with H95 is greatly relieved in the twist-boat conformer (Figure 3b, yellow structure).

Moreover, favorable CH−π interactions, indicated by magenta dashed line, are present between equatorial methyl groups and nearby aromatic residues—F177 in the CB_1 case (Figure 3a) and F94 in the CB_2 case (Figure 3b). The distances from the methyl proton of (9*R*)-HHC to the aromatic π-system of F177 and F94 are 3.1 and 3.2 Å, respectively. In the representative binding poses obtained from MD simulations (see the SI for details), these CH−π interactions are consistently preserved. We believe that such noncovalent interactions contribute to the enhanced stability of equatorial methyl groups compared to axial ones.

We also compared the docking of three ligands that possess an equatorial C9 methyl group: Δ^9-THC, (9*R*)-HHC (favored chair conformation), and the disfavored twist-boat form of (9*S*)-HHC (Figure 4). In the case of either the CB_1 or CB_2 active site (Figure 4a or b, respectively), very similar interactions are seen. In fact, the ligands in the binding site are nearly superimposable. Thus, we surmised that the binding of (9*S*)-HHC to CB_1 and CB_2 may arise through its twist-boat conformer that positions the C9 methyl group in an equatorial position, despite the fact that the twist-boat conformer is higher in energy than the chair conformer outside of the binding pocket (see Figure 1b). Indeed, binding free energy calculations further support this proposition, as we will discuss below (see Table 1).

Molecular Dynamics (MD) Simulations. MD simulations were carried out to refine the binding pose. We first conducted MD simulations starting from the crystal structure of CB_1 (PDB ID: 5XRA).[33] The binding pose remains virtually unchanged throughout the MD simulation, with the root-mean-square deviation (RMSD) between the original crystal ligand AM11542 and the ligand after the simulation being only 0.476 Å (Figure S1). Then, MD simulations were performed on docked structures of Δ^9-THC, (9*R*)-HHC, and (9*S*)-HHC, where the docking pose as shown in Figures 3 and 4 is generally preserved (Figure S2), while the long aliphatic chain of the cannabinoid is adjusted to a lower-energy conformation. We performed 3 independent 1000 ns MD simulations on each receptor−ligand complex. For Δ^9-THC, a low-energy half-chair conformation (equatorial C9 methyl group) is maintained within the receptor's active site throughout the entire simulation (Figures S2 and S3).

During the MD simulations, we were particularly interested in the conformation of the cyclohexyl ring for (9*R*)-HHC and (9*S*)-HHC. This could be gauged by monitoring the C6a−C7−C8−C9 dihedral angle (Scheme 1). When this dihedral angle is around 54 degrees, the cyclohexyl ring of the ligand adopts a chair conformation; when the dihedral angle is roughly −20 degrees, the ligand exists in a twist-boat conformation. Depending on which isomer of HHC is being evaluated, the conformation will then dictate the positioning of the C9 methyl group (axial or equatorial).

Scheme 1. Schematic Illustration of the C6a−C7−C8−C9 Dihedral Angle Monitored during the MD Simulation

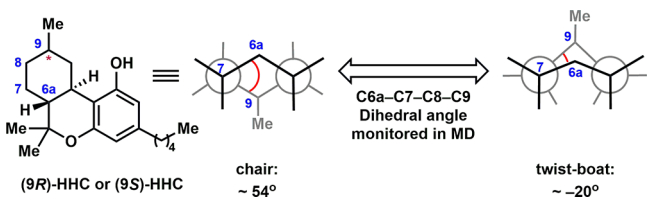

https://doi.org/10.1021/acschembio.5c00399
ACS Chem. Biol. XXXX, XXX, XXX−XXX

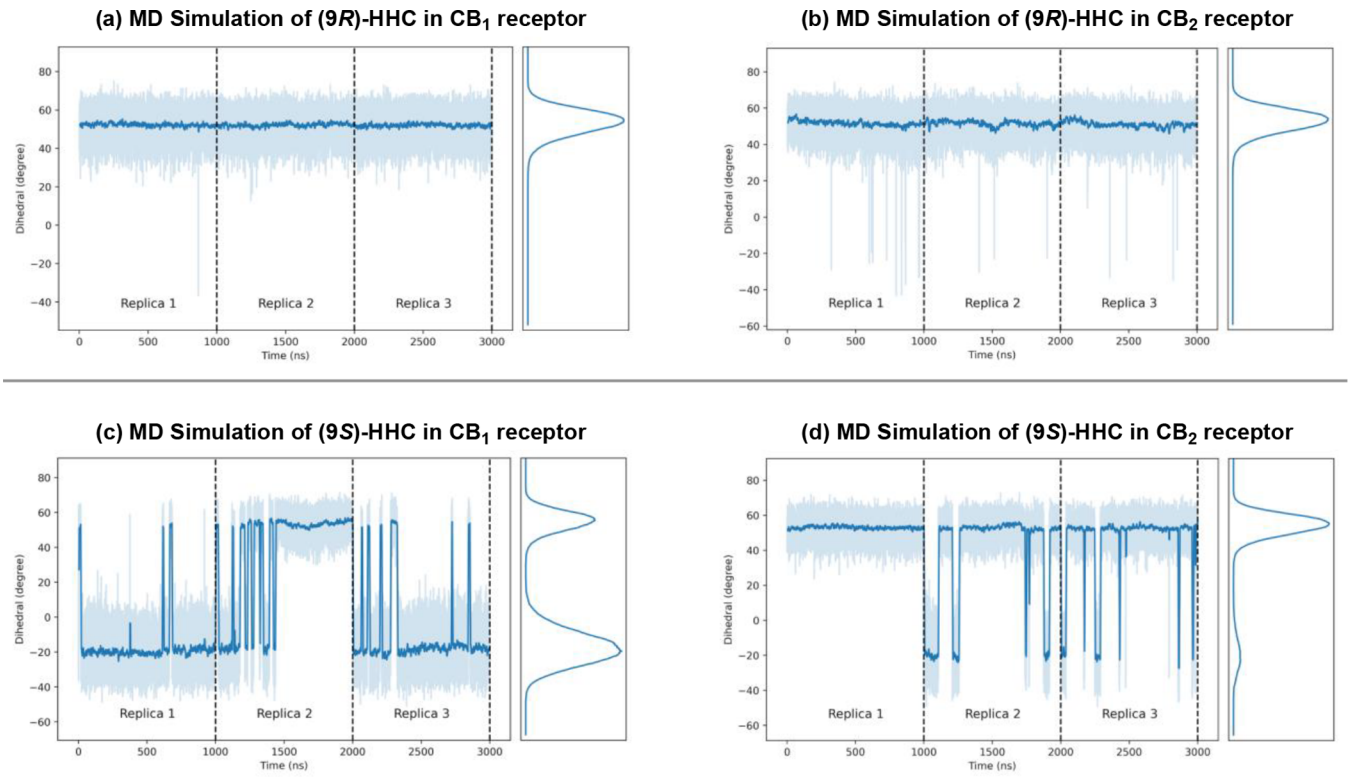

Figure 5. MD simulations on the receptor−ligand complexes for (a) (9*R*)-HHC in CB_1, (b) (9*R*)-HHC in CB_2, (c) (9*S*)-HHC in CB_1, and (d) (9*S*)-HHC in CB_2.

Table 1. Experimental and ProFESSA FEP Computed Binding Affinities for (9*R*)-HHC and (9*S*)-HHC

ligand	K_i CB_1 (nM)	$\Delta\Delta G_{exp}$ (kcal/mol)	$\Delta\Delta G_{cal}$ (kcal/mol)	K_i CB_2 (nM)	$\Delta\Delta G_{exp}$ (kcal/mol)	$\Delta\Delta G_{cal}$ (kcal/mol)
(9*R*)-HHC	15	0.0	0.0	13	−0.1	−0.1
(9*S*)-HHC	176	1.5	1.6 ± 0.3	105	1.2	1.4 ± 0.2

As shown in Figure 5a,b, for (9*R*)-HHC binding, the monitored dihedral angle remains consistently around 54 degrees throughout the simulation for both the CB_1 and CB_2 receptors. This indicates that the ligand prefers to adopt a chair conformation in the receptor's active site, where the C9 methyl group is positioned in an equatorial orientation. This is analogous to what is seen for the unbound ligand (Figure 1b).

In contrast, when (9*S*)-HHC binds to either CB_1 or CB_2, the dihedral angle fluctuates between approximately 54 degrees and −20 degrees during the simulation (Figure 5c,d). This indicates that (9*S*)-HHC exists in equilibrium between the chair (axial C9 methyl) and twist-boat conformations (equatorial C9 methyl). These findings are notable, as in the unbound state, the twist-boat form of (9*S*)-HHC is 2.4 kcal/mol higher in energy than the chair conformation (see Figure 1b). Therefore, while the resting state of (9*S*)-HHC is expected to be the chair form, an unfavorable conformational change of the cyclohexyl ring to the twist-boat form is necessary for binding, as this change alleviates steric clashing with nearby residues as discussed earlier (see Figure 3). The presence of the chair conformer of (9*S*)-HHC (axial C9 methyl) explains why (9*S*)-HHC is a less favorable ligand for CB_1 and CB_2 compared to (9*R*)-HHC.

We also performed calculations to assess the binding energies for (9*R*)-HHC and (9*S*)-HHC (see the SI for binding energy calculations for Δ^9-THC). Such calculations have not been reported previously and require the evaluation of different methods. Calculations obtained using molecular mechanics Poisson−Boltzmann surface area (MM/PBSA)[43−45] methods show promise, but also suggest some limitations for calculating HHC binding to the cannabinoid receptors, as provided in the SI. To better estimate the relative binding free energy between (9*R*)-HHC and (9*S*)-HHC, we conducted alchemical simulations using ProFESSA, a free energy perturbation method developed by York and co-workers.[46] Thus, (9*R*)-HHC was allowed to transform to its epimer (9*S*)-HHC in the simulations conducted for both CB_1 and CB_2 receptors. These simulations were initiated with the chair conformation of (9*R*)-HHC, while allowing conversion to the twist-boat conformation of (9*S*)-HHC during the alchemical process. For the CB_1 case, during the transformation from (9*R*)-HHC to (9*S*)-HHC, we observed the interconversion between the chair form of (9*S*)-HHC with its twist-boat conformation. Specifically, in three independent runs, the chair conformation was dominant in one run, while the twist-boat conformation was observed in the other two. This indicates that within the active site of CB_1, (9*S*)-HHC exists in equilibrium between the chair and twist-boat conformations, consistent with the MD observations (Figure 5c). In contrast, for the CB_2 case, in all of the replicated simulations, the ligand structure transitioned smoothly from the chair conformation of (9*R*)-HHC to the chair conformation of (9*S*)-HHC. This observation aligns well with the MD results, which show that the chair form of (9*S*)-

https://doi.org/10.1021/acschembio.5c00399
ACS Chem. Biol. XXXX, XXX, XXX−XXX

HHC is dominant over the twist-boat conformation in the CB_2 case (Figure 5d), leading to poorer receptor binding.

Table 1 shows a comparison of experimental binding affinities for (9*R*)-HHC and (9*S*)-HHC to calculated binding affinities using ProFESSA FEP. We were delighted to find reasonable correlations between the relative binding affinities. For binding to the CB_1 receptor, the experimental and predicted energies for the (9*R*)-HHC isomer match, and there is also good agreement for the (9*S*)-HHC isomer ($\Delta\Delta G_{exp}$ = 1.5 kcal/mol vs $\Delta\Delta G_{calc}$ = 1.6 ± 0.3 kcal/mol). Similar trends are seen for binding to the CB_2 receptor, as shown, with our results collectively showing that ProFESSA FEP can be used to gain a qualitative sense of the relative binding of (9*R*)-HHC to (9*S*)-HHC for both the CB_1 and CB_2 receptors. This method should prove useful for calculating the relative binding affinities of other cannabinoids in the future.

CONCLUSIONS

We have performed a computational study of the emerging cannabinoids HHCs. These compounds are notable as they are available for recreational use in the United States but were recently classified as Schedule II under an international treaty. Moreover, the two HHC isomers in commercial products, (9*R*)-HHC and (9*S*)-HHC, are typically present in variable amounts, which is notable as these epimers have been shown to have different binding affinities to the CB_1 and CB_2 receptors.

Using a combination of molecular docking and molecular dynamics simulations, we identified the key interactions in the active sites. In addition, we have found a surprising explanation for the difference in binding affinities of (9*R*)-HHC and (9*S*)-HHC to the cannabinoid receptors related to conformational effects. (9*R*)-HHC exists primarily in a chair conformation and binds favorably to both CB_1 and CB_2 in this same chair conformation, analogous to the binding of Δ^9-THC to the cannabinoid receptors. This explains the strong binding affinity of (9*R*)-HHC and why its binding affinity is similar to that of Δ^9-THC. However, the conformational effects for (9*S*)-HHC are more complex. In the unbound state, (9*S*)-HHC exists primarily in the chair conformation. However, for both CB_1 and CB_2, (9*S*)-HHC exists in equilibrium between the chair and twist-boat conformations within the receptor's active site. The former of these is thought not to bind favorably to the cannabinoid receptor, while the twist-boat conformation binds more favorably. The difference in binding between these two conformers is attributed to an accompanying change in the orientation of the C9 methyl group. The MD simulations not only reveal the key conformational effects but also correctly predict the relative binding affinities of (9*R*)-HHC and (9*S*)-HHC when using ProFESSA FEP.

These studies provide insight into how HHCs bind to the cannabinoid receptors and are expected to enable the design and discovery of modified cannabinoids that display improved binding, desirable selectivities, and potential therapeutic activity.

ASSOCIATED CONTENT

Supporting Information

The Supporting Information is available free of charge at https://pubs.acs.org/doi/10.1021/acschembio.5c00399.

Additional molecular docking and molecular dynamics results. Coordinates and energies of DFT-computed stationary points (PDF)

AUTHOR INFORMATION

Corresponding Authors

Yi Tang − *Department of Chemistry and Biochemistry and Department of Chemical and Biomolecular Engineering, University of California, Los Angeles, California 90095, United States;* orcid.org/0000-0003-1597-0141; Email: yitang@ucla.edu

Neil K. Garg − *Department of Chemistry and Biochemistry, University of California, Los Angeles, California 90095, United States;* orcid.org/0000-0002-7793-2629; Email: neilgarg@ucla.edu

K. N. Houk − *Department of Chemistry and Biochemistry and Department of Chemical and Biomolecular Engineering, University of California, Los Angeles, California 90095, United States;* orcid.org/0000-0002-8387-5261; Email: houk@chem.ucla.edu

Authors

Pan-Pan Chen − *Department of Chemistry and Biochemistry, University of California, Los Angeles, California 90095, United States*

Meng Duan − *Department of Chemistry and Biochemistry, University of California, Los Angeles, California 90095, United States*

Qingyang Zhou − *Department of Chemistry and Biochemistry, University of California, Los Angeles, California 90095, United States*

Fang Liu − *Department of Chemistry and Biochemistry, University of California, Los Angeles, California 90095, United States;* orcid.org/0000-0002-0046-8434

Complete contact information is available at: https://pubs.acs.org/10.1021/acschembio.5c00399

Notes

The authors declare no competing financial interest.

ACKNOWLEDGMENTS

We are grateful to the California Department of Cannabis Control (Grant Agreement Number: 93414) for financial support of this research. We thank Allison Hands, Jiaming Ding, and Giulianna Miseo (UCLA) for insightful discussions. Calculations were performed on the IDRE Hoffman2 cluster at the University of California, Los Angeles, and Expanse at SDSC through allocation CHE040014 from the Advanced Cyberinfrastructure Coordination Ecosystem: Services & Support (ACCESS) program.

REFERENCES

(1) Lampe, J. R. *Recent Developments in Marijuana Law*. Congressional Research Service, Dec. 6, 2022. Available via the Internet at: https://crsreports.congress.gov/product/pdf/LSB/LSB10859 (accessed July 19, 2025).

(2) Sacco, L. N. *Evolution of Marijuana as a Controlled Substance and the Federal-State Policy Gap*. Congressional Research Service, April 7, 2022. Available via the Internet at: https://crsreports.congress.gov/product/pdf/R/R44782 (accessed July 19, 2025).

(3) Erickson, B. E. Cannabis research bill clears U.S. Congress. *Chem. Eng. News*, **2022**. Available via the Internet at: https://cen.acs.

org/biological-chemistry/natural-products/Cannabis-research-bill-clears-US/100/i43 (accessed July 19, 2025).
(4) Huang, D.; Forbes, C. R.; Garg, N. K.; Darzi, E. R. A Cannabinoid Fuel Cell Capable of Producing Current by Oxidizing Δ^9-Tetrahydrocannabinol. *Org. Lett.* **2022**, *24*, 6705−6710.
(5) Darzi, E. R.; Garg, N. K. Electrochemical Oxidation of Δ^9-Tetrahydrocannabinol: A Simple Strategy for Marijuana Detection. *Org. Lett.* **2020**, *22*, 3951−3955.
(6) Iversen, L. The pharmacology of delta-9-Tetrahydrocannabinol (THC). In *The Science of Marijuana*, 3rd ed.; Oxford University Press: 2018; pp 22−C2.F7.
(7) Qureshi, M. N.; Kanwal, F.; Siddique, M.; Inayat-ur-Rahman; Akram, M. Estimation of Biologically Active Cannabinoids in Cannabis Indica by Gas Chromatography-mass Spectrometry (GC-MS). *World Appl. Sci. J.* **2012**, *19*, 918−923.
(8) Collins, A. C.; Ramirez, G. A.; Tesfatsion, T. T.; Ray, K. P.; Cruces, W. Synthesis and Characterization of the Diastereomers of HHC and H4CBD. *Nat. Prod. Commun.* **2023**, *18*, 1−6.
(9) Jørgensen, C. F.; Rasmussen, B. S.; Linnet, K.; Thomsen, R. Emergence of Semi-synthetic Cannabinoids in Cannabis Products Seized in Eastern Denmark over a 6-year Period. *J. Forensic Sci.* **2024**, *69*, 2009−2017.
(10) Shahbazi, F.; Grandi, V.; Banerjee, A.; Trant, J. F. Cannabinoids and Cannabinoid Receptors: The Story so Far. *iScience* **2020**, *23*, No. 101301.
(11) Nasrallah, D. J.; Garg, N. K. Studies Pertaining to the Emerging Cannabinoid Hexahydrocannabinol (HHC). *ACS Chem. Biol.* **2023**, *18*, 2023−2029.
(12) Persson, M.; Kronstrand, R.; Evans-Brown, M.; Green, H. In vitro Activation of the CB_1 Receptor by the Semi-synthetic Cannabinoids Hexahydrocannabinol (HHC), Hexahydrocannabinol Acetate (HHC-O) and Hexahydrocannabiphorol (HHC-P). *Drug Test Anal.* **2025**, *17*, 487−493.
(13) Bottinelli, C.; Baradian, P.; Poly, A.; Hoizey, G.; Chatenay, C. Identification and Quantification of Both Isomers of Hexahydrocannabinol, (9*R*)-hexahydrocannabinol and (9*S*)-hexahydrocannabinol, in Three Different Matrices by Mass Spectrometry. *Rapid Commun. Mass Spectrom.* **2024**, *38*, No. e9711.
(14) Sams, R. A. *Analysis of Hexahydrocannabinols: Eliminating Uncertainty in its identification*. https://api.semanticscholar.org/CorpusID:259319262 (accessed Nov 3, 2023).
(15) Joad Costa, A. HHC Classified as "Schedule II" by the Commission on Narcotic Drugs and Drug Enforcement, *Canna Reporter*, March 12, 2025.
(16) Marusich, J. A.; Prioleau, C.; Akinfiresoye, L. R. Cannabimimetic and Discriminative Stimulus Effects of Hexahydrocannabinols in Mice. *Journal of Psychopharmacology.* **2025**, *39*, 736−743.
(17) Thomsen, R.; Axelsen, T. M.; Løkken, N.; et al. Prolonged Sedation and Unconsciousness after Intoxication with the Novel Semisynthetic Cannabinoid Hexahydrocannabioctyl (HHC-C8): Two Case Descriptions. *Toxicol. Rep.* **2025**, *14*, No. 101912.
(18) Hundertmark, M.; Besch, L.; Röhrich, J.; Germerott, T.; Wunder, C. Characterising a New Cannabis Trend: Extensive Analysis of Semi-Synthetic Cannabinoid-Containing Seizures From Germany. *Drug Testing and Analysis* **2025**, *0*, 1−14.
(19) Zawatsky, C. N.; Mills-Huffnagle, S.; Augusto, C. M.; Vrana, K. E.; Nyland, J. E. Cannabidiol-Derived Cannabinoids: The Unregulated Designer Drug Market Following the 2018 Farm Bill. *Med. Cannabis Cannabinoids.* **2024**, *7*, 10−18.
(20) An, D.; Peigneur, S.; Hendrickx, L. A.; Tytgat, J. Targeting Cannabinoid Receptors: Current Status and Prospects of Natural Products. *Int. J. Mol. Sci.* **2020**, *21*, 5064.
(21) Lutz, B. Neurobiology of Cannabinoid Receptor Signaling. *Dialogues in Clinical Neuroscience* **2020**, *22*, 207−222.
(22) Adams, R.; Pease, D. C.; Cain, C. K.; Clark, J. H. Structure of Cannabidiol. VI. Isomerization of Cannabidiol to Tetrahydrocannabinol, a Physiologically Active Product. Conversion of Cannabidiol to Cannabinol. *J. Am. Chem. Soc.* **1940**, *62*, 2402−2405.
(23) Computational details are included in the Supporting Information.
(24) Archer, R. A.; Boyd, D. B.; Demarco, P. V.; Tyminski, I. J.; Allinger, N. L. Structural Studies of Cannabinoids. Theoretical and Proton Magnetic Resonance Analysis. *J. Am. Chem. Soc.* **1970**, *92*, 5200−5206.
(25) Reggio, P. H.; Greer, K. V.; Cox, S. M. The Importance of the Orientation of the C9 Substituent to Cannabinoid Activity. *J. Med. Chem.* **1989**, *32*, 1630−1635.
(26) Reggio, P. H.; Panu, A. M.; Miles, S. Characterization of a Region of Steric Interference at the Cannabinoid Receptor using the Active Analog Approach. *J. Med. Chem.* **1993**, *36*, 1761−1771.
(27) Mechoulam, R.; Lander, N.; Varkony, T. H.; Kimmel, I.; Becker, O.; Ben-Zvi, Z.; et al. Stereochemical Requirements for Cannabinoid Activity. *J. Med. Chem.* **1980**, *23*, 1068−1072.
(28) Zhao, Y.; Truhlar, D. G. The M06 Suite of Density Functionals for Main Group Thermochemistry, Thermochemical Kinetics, Noncovalent Interactions, Excited States, and Transition Elements: Two New Functionals and Systematic Testing of Four M06-class Functionals and 12 Other Functionals. *Theor. Chem. Acc.* **2008**, *120*, 215−241.
(29) Zhao, Y.; Truhlar, D. G. Density Functionals with Broad Applicability in Chemistry. *Acc. Chem. Res.* **2008**, *41*, 157−167.
(30) Legault, C. Y. *CYLview, version 1.0b*; Université de Sherbrooke: 2009 (http://www.cylview.org).
(31) Eliel, E. L.; Wilen, S. H.; Mander, L. N. *Stereochemistry of Organic Compounds*; Wiley: United Kingdom, 1994.
(32) Of note, this 2.4 kcal/mol difference in chair versus twist-boat conformational energies for (9*S*)-HHC contrasts with the usual 5.5 kcal/mol difference for cyclohexane. Clayden, J. *Organic chemistry (2nd ed.)*; Oxford: 2003; p 373. ISBN 9780191666216.
(33) Hua, T.; Vemuri, K.; Nikas, S. P.; Laprairie, R. B.; Wu, Y.; Qu, L.; Pu, M.; Korde, A.; Jiang, S.; Ho, J. H.; Han, G. W.; Ding, K.; Li, X.; Liu, H.; Hanson, M. A.; Zhao, S.; Bohn, L. M.; Makriyannis, A.; Stevens, R. C.; Liu, Z. J. Crystal Structures of Agonist-bound Human Cannabinoid Receptor CB_1. *Nature* **2017**, *547*, 468−471.
(34) Hua, T.; Li, X.; Wu, L.; Iliopoulos-Tsoutsouvas, C.; Wang, Y.; Wu, M.; Shen, L.; Johnston, C. A.; Nikas, S. P.; Song, F.; Song, X.; Yuan, S.; Sun, Q.; Wu, Y.; Jiang, S.; Grim, T. W.; Benchama, O.; Stahl, E. L.; Zvonok, N.; Zhao, S.; Bohn, L. M.; Makriyannis, A.; Liu, Z. J. Activation and Signaling Mechanism Revealed by Cannabinoid Receptor-Gi Complex Structures. *Cell* **2020**, *180*, 655−665.e18.
(35) Linciano, P.; Citti, C.; Luongo, L.; Belardo, C.; Maione, S.; Vandelli, M. A.; Forni, F.; Gigli, G.; Laganà, A.; Montone, C. M.; Cannazza, G. Isolation of a High-Affinity Cannabinoid for the Human CB1 Receptor from a Medicinal *Cannabis sativa* Variety: Δ^9-Tetrahydrocannabutol, the Butyl Homologue of Δ^9-Tetrahydrocannabinol. *J. Nat. Prod.* **2020**, *83*, 88−98.
(36) Jung, S. W.; Cho, A. E.; Yu, W. Exploring the Ligand Efficacy of Cannabinoid Receptor 1 (CB1) using Molecular Dynamics Simulations. *Sci. Rep.* **2018**, *8*, 13787.
(37) Thorsen, T. S.; Kulkarni, Y.; Sykes, D. A.; et al. Structural basis of THC analog activity at the Cannabinoid 1 receptor. *Nat. Commun.* **2025**, *16*, 486.
(38) Ji, S.; Yang, W.; Yu, W. Understanding the role of the CB1 toggle switch in interaction networks using molecular dynamics simulation. *Sci. Rep.* **2021**, *11*, 22369.
(39) Haghdoost, M.; López de los Santos, Y.; Brunstetter, M.; Ferretti, M. L.; Roberts, M.; Bonn-Miller, M. O. Using In Silico Molecular Docking to Explain Differences in Receptor Binding Behavior of HHC and THCV Isomers: Revealing New Binding Modes. *Pharmaceuticals* **2024**, *17*, 637.
(40) Eberhardt, J.; Santos-Martins, D.; Tillack, A. F.; Forli, S. AutoDock Vina 1.2.0: New Docking Methods, Expanded Force Field, and Python Bindings. *J. Chem. Inf. Model.* **2021**, *61*, 3891−3898.
(41) Trott, O.; Olson, A. J. AutoDock Vina: Improving the Speed and Accuracy of Docking with a New Scoring Function, Efficient Optimization, and Multithreading. *J. Comput. Chem.* **2010**, *31*, 455−461.

https://doi.org/10.1021/acschembio.5c00399
ACS Chem. Biol. XXXX, XXX, XXX−XXX

(42) Huang, S.; Xiao, P.; Sun, J. Structural Basis of Signaling of Cannabinoids Receptors: Paving a Way for Rational Drug Design in Controling Multiple Neurological and Immune Diseases. *Signal Transduction Targeted Ther.* **2020**, *5*, 127.
(43) Genheden, S.; Ryde, U. The MM/PBSA and MM/GBSA Methods to Estimate Ligand-Binding Affinities. *Expert Opin. Drug Discovery* **2015**, *10*, 449−461.
(44) Yang, J.-F.; Williams, A. H.; Penthala, N. R.; Prather, P. L.; Crooks, P. A.; Zhan, C.-G. Binding Modes and Selectivity of Cannabinoid 1 (CB1) and Cannabinoid 2 (CB2) Receptor Ligands. *ACS Chem. Neurosci.* **2020**, *11*, 3455−3463.
(45) King, E.; Aitchison, E.; Li, H.; Luo, R. Recent Developments in Free Energy Calculations for Drug Discovery. *Front. Mol. Biosci.* **2021**, *8*, No. 712085.
(46) Ganguly, A.; Tsai, H.-C.; Fernández-Pendás, M.; Lee, T.-S.; Giese, T. J.; York, D. M. AMBER Drug Discovery Boost Tools: Automated Workflow for Production Free-Energy Simulation Setup and Analysis (ProFESSA). *J. Chem. Inf. Model.* **2022**, *62*, 6069−6083.

https://doi.org/10.1021/acschembio.5c00399
ACS Chem. Biol. XXXX, XXX, XXX−XXX